Nanoscale Advances

ROYAL SOCIETY OF CHEMISTRY

PAPER

View Article Online
View Journal | View Issue

Cite this: *Nanoscale Adv.*, 2020, **2**, 4085

Is carboxylation an efficient method for graphene oxide functionalization?†

Shi Guo,[a] Jésus Raya,[b] Dingkun Ji,[a] Yuta Nishina,[cd] Cécilia Ménard-Moyon[a] and Alberto Bianco*[a]

Graphene oxide (GO) is one of the most popular materials applied in different research areas thanks to its unique properties. The application of GO requires well-designed protocols to introduce different functionalities on its surface, exploiting the oxygenated groups already present. Due to the complex and unstable chemical environment on the GO surface, it is recommended to perform the functionalization under mild conditions. The carboxylation of GO is a widely used method to introduce additional carboxylic acids, which could be further modified through amidation or esterification reactions. The strategy already reported in the literature requires harsh conditions (excess amount of sodium hydroxide). GO is readily reduced under basic conditions, but the reduction of GO during the carboxylation is barely studied. In this work, we performed the carboxylation using chloroacetic acid with different amounts of sodium hydroxide and characterized the functionalized GO with various techniques. The carboxylated GO was exploited to develop a double functionalization approach combining an epoxide ring opening reaction and an amidation. The results showed that strong basic conditions were necessary to derivatize GO. Nevertheless, these conditions resulted in a partial reduction of GO and some functionalities on GO were removed during the reaction, thus reducing the total efficiency of the functionalization in comparison to an epoxide ring opening reaction, indicating that carboxylation is not an efficient approach for the functionalization of GO.

Received 16th May 2020
Accepted 8th July 2020

DOI: 10.1039/d0na00561d

rsc.li/nanoscale-advances

Introduction

Over the past two decades, GO has attracted large interest and is one of the most popular nanomaterials with great potential applications in different fields covering energy storage,[1,2] antibacterial agents,[3,4] biosensing,[5] diagnosis and therapy,[6–9] and artificial muscles.[10] GO is the oxidized form of graphene, usually prepared by the oxidation of graphite using strong acid treatments.[11,12] It consists of a hexagonal ring-based carbon network with abundant oxygen-containing functional groups such as epoxides and hydroxyls on the basal plane, as well as carboxyl and carbonyl groups at the edges, along with limited localized graphitic domains.[13] These oxygenated functional groups endow GO with unique properties including high dispersibility in water,[14] good biodegradability,[15,16] optical transparency and photoluminescence quenching.[17,18] The high surface area of GO allows adsorption of a large amount of drugs,[6,19] RNA[20,21] or nanoparticles,[22] while bioactive molecules can also be covalently conjugated *via* the oxygenated groups.[23] The possibility of grafting functionalities onto the surface of GO greatly extends its application to different areas.[24–27] Compared to noncovalent complexation, covalent functionalization enables us to prepare more stable conjugates and minimize the release of molecules adsorbed onto the GO surface, especially for biological applications. Several strategies have been reported to functionalize GO covalently by targeting different functional groups such as carboxylic acids,[28] epoxide rings[29] and hydroxyl groups[30–33] allowing the development of approaches for double functionalization.[31,32,34] However, the derivatization of the carboxylic acids leads to very low loading efficiency compared to the functionalization of the hydroxyl and epoxide moieties, due to the limited amount of COOH on GO.[29] Therefore, a higher amount of carboxylic acids would broaden the possibilities for multi-functionalization of GO with a high loading efficiency. Because of their large surface area, two-dimensional materials have a limited amount of functional groups at the edges in comparison with the basal plane. In order to increase the amount of carboxyl groups on GO, a method of carboxylation was developed through the derivatization of hydroxyls with chloroacetic acid in the presence of sodium hydroxide.[35–37] The

[a]*CNRS, Immunology, Immunopathology and Therapeutic Chemistry, UPR3572, University of Strasbourg, ISIS, 67000 Strasbourg, France*

[b]*Membrane Biophysics and NMR, Institute of Chemistry, UMR 7177, University of Strasbourg, Strasbourg, France*

[c]*Graduate School of Natural Science and Technology, Okayama University, Tsushimanaka, Kita-ku, Okayama, 700-8530, Japan*

[d]*Research Core for Interdisciplinary Sciences, Okayama University, Tsushimanaka, Kita-ku, Okayama, 700-8530, Japan. E-mail: a.bianco@ibmc-cnrs.unistra.fr*

† Electronic supplementary information (ESI) available. See DOI: 10.1039/d0na00561d

prepared carboxylated GO was further derivatized with amine-containing functionalities by amidation.[34,36,38] However, it was reported that the use of a strong base often causes deoxygenation resulting in the partial reduction of GO,[39,40] thus changing its properties and influencing the efficiency of the functionalization. Although some articles already reported the partial reduction of GO during carboxylation using chloroacetic acid and sodium hydroxide,[35,41] the effect of this deoxygenation on the functionalization efficiency of GO is still not clear. Under most conditions, a wide concentration range of sodium hydroxide solutions was used from 123 mM to 4 M, with 3 M being the most commonly used.

To clarify the impact of a strong alkaline solution on GO, we prepared carboxylated GO using different molarities of sodium hydroxide and performed characterization by X-ray photoelectron spectroscopy (XPS), thermogravimetric analysis (TGA), transmission electron microscopy (TEM), magic angle spinning (MAS) NMR and FT-IR spectroscopy. The introduction of the carboxylates was observed along with a partial reduction of GO. The efficiency of multifunctionalization of the carboxylated GO was evaluated by the epoxide ring opening and amidation reaction.

Results and discussion

(1) Carboxylation of GO with high amount of sodium hydroxide

Large GO flakes (30 μm) were prepared following a modified Hummers method. By using a jet mill with a 0.1 mm nozzle, GO with an average lateral size of 1 μm was obtained.[31] We first derivatized GO with chloroacetic acid under strongly basic conditions following the protocol published by other groups to increase the amount of carboxylic acids.[37] Briefly, the pristine GO was dispersed in 3 M sodium hydroxide solution followed by the immediate addition of chloroacetic acid (Scheme 1). After washing and dialysis, the resulting GO **1** was characterized by XPS, TGA, FT-IR and TEM.

XPS provides information on the chemical composition of the surface of GO (Fig. 1). The atomic percentage compositions of the pristine GO and GO **1** were measured (Fig. 1a and c, respectively), presenting a C/O ratio of 2.6 for the starting GO and 3.0 for GO **1**. The increase of the C/O ratio after carboxylation was certainly due to a partial reduction of GO,[44] indicating that some of the oxygen-containing functional groups were removed during the reaction. The reduction of GO was also supported by the analysis of the high resolution C 1s spectra. The C 1s spectrum of the pristine GO exhibited two major peaks assigned to the C–C bond at 284.8 eV and the C–O bond from alcohols and epoxides at 286.6 eV (Fig. 1b). The shoulder in the 288.1 to 289.1 eV region could be deconvoluted into two components, the carboxyl groups in the region from 288.7 eV to 289.1 eV and the carbonyl groups from 288.1 eV to 288.3 eV. The C 1s spectrum changed significantly after the reaction (Fig. 1d). The carboxyl groups on GO increased from 3.9% to 6.2%, proving the successful modification of GO with carboxylic acids. However, a significant decrease of the C–O component from 44.0% to 28.7% was also observed, confirming the partial reduction of GO during the reaction.[45] Some labile oxygenated groups and oxidative debris[46] were likely removed from the GO surface during the treatment with sodium hydroxide. Some of the epoxide rings were probably opened by OH^- and the hydroxyl groups could be further reduced by OH^- with the assistance of Na^+ and water molecules, resulting in the formation of CO_2, vacancy defects and extension of conjugation, as previously reported.[39,47] The partial reduction of GO affects its intrinsic properties and may decrease the loading of molecules conjugated to the COOH groups. The high resolution O 1s peak was deconvoluted into three components: C=O (531.4–530.3 eV), C–O (533.0–532.0 eV) and H_2O (535.2–534.8 eV). The increase of the C=O component from 5.0% to 5.7% after carboxylation was not very significant, probably due to the contribution of the chloroacetic acid moiety to both peaks (Fig. S1†).

The reduction of GO was corroborated by thermogravimetric analysis under an inert atmosphere (Fig. 2a). The TGA curve of the pristine GO showed two main weight losses due to (i) physisorbed water (30–100 °C) and (ii) decomposition of labile oxygenated groups (~150–200 °C). As evident in Fig. 2a, the TGA curve of GO **1** displayed a higher thermal stability in the 150–200 °C region and the total weight loss was lower.[47] The increase of the thermal stability could be attributed to the partial reduction of GO by removal of some labile oxygen-containing groups.

The GO samples were characterized by attenuated total reflectance (ATR) FT-IR spectroscopy (Fig. 2b). The spectrum of the pristine GO displayed a broad peak around 3400 cm^{-1}

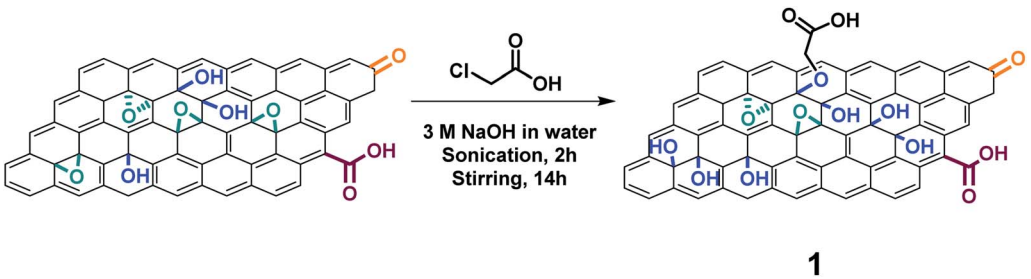

1

Scheme 1 Carboxylation reaction on GO. For the sake of clarity, only one hydroxyl group is derivatized and the epoxide rings are closed. The epoxide ring opening by sodium hydroxide is under an equilibrium and some of the C–O^- groups can close again to form a ring.[42,43]

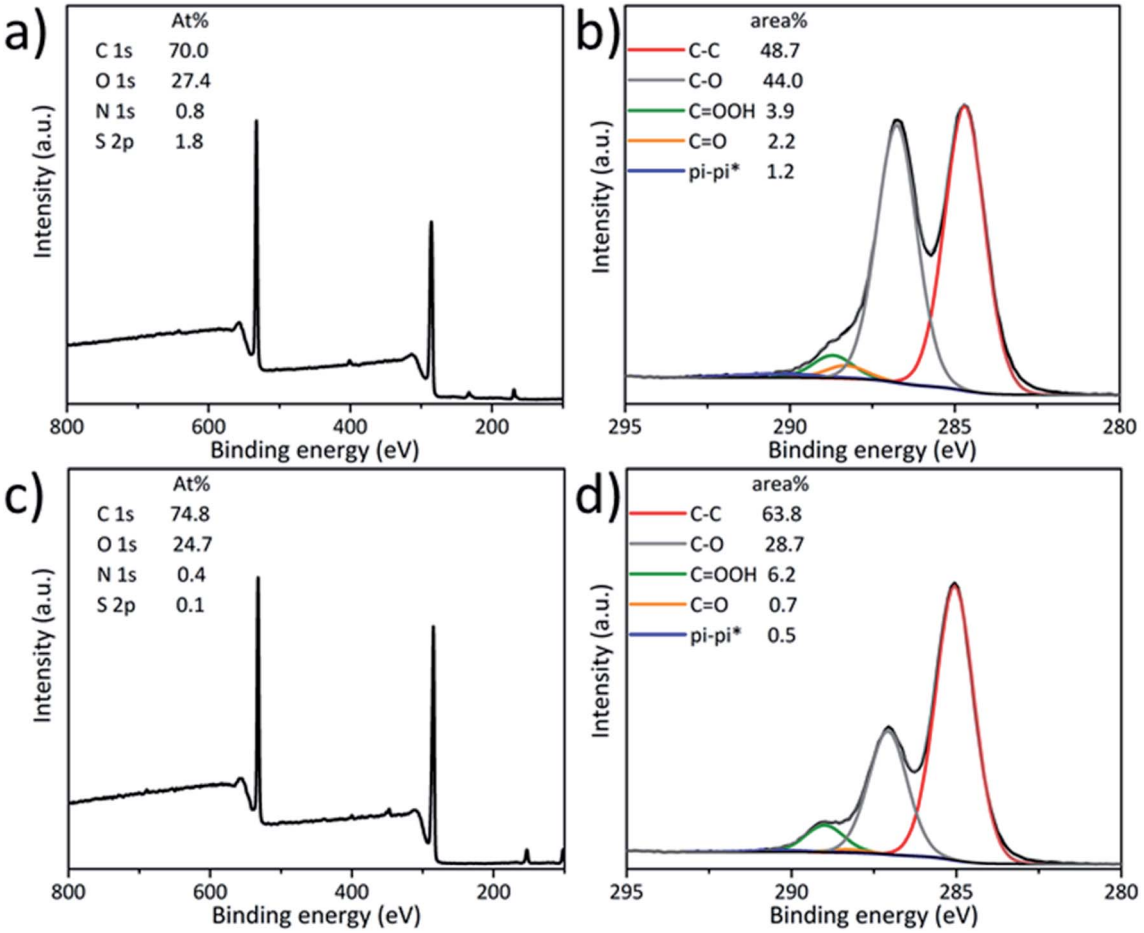

Fig. 1 XPS survey spectra (a and c) and high resolution C 1s (b and d) spectra of pristine GO (top row) and GO **1** (bottom row).

assigned to the O–H stretching of the adsorbed water and the hydroxyl functionalities of GO.[48] The band at 1723 cm^{-1} was attributed to the stretching of C=O groups. The peak at 1619 cm^{-1} corresponded to the H–O–H bending vibration of water molecules and the skeletal C=C bond vibrations of the graphitic domains. The band at 1371 cm^{-1} was assigned to the O–H bending vibration. The C–O–C vibration band of the epoxides was located at 1232 cm^{-1} and the peak at 1143 cm^{-1} was assigned to the C–O stretching. After the carboxylation, the stretching band of C=O at 1723 cm^{-1} was still present as well as the O–H stretching at ~3400 cm^{-1}.

The morphology of GO was characterized by TEM (Fig. S2†). The GO sheets have an average lateral dimension of around 1 μm and a wavy shape with folded edges. After carboxylation, the morphology of GO was not affected.

Although the carboxylation method using chloroacetic acid and sodium hydroxide has been widely used for GO surface modification, the partial reduction of the material was never clearly mentioned. On the other hand, the reduction of GO in strongly alkaline solution at room temperature has been reported by several groups,[39,40,46,47] and it has been proved as an efficient way to produce reduced GO.[38]

To better understand the effect of the partial reduction on GO functionalization, we combined an epoxide ring opening reaction and the carboxylation of GO followed by an amidation using *O*-(2-aminoethyl)-*O*′-[2-(Boc-amino)ethyl]decaethylene glycol (BocNH-PEG_{10}-NH_2) in the presence of activating agents (EDC/NHS) to achieve the double functionalization (Scheme 2). The colorimetric Kaiser test was used to determine the amount of amino-PEG groups grafted onto GO after Boc deprotection.[30,49,50] The epoxide ring opening reaction was first performed since the epoxides easily react with amines through a nucleophilic addition forming C–N bonds and new hydroxyl groups,[29] which can be further derivatized with chloroacetic acid. For this purpose, the pristine GO was mixed with BocNH-PEG_{10}-NH_2 in water and stirred for 3 days at room temperature (Scheme 2). After washing and dialysis, GO **2** was obtained. The amount of primary amines on GO **2** was assessed by the Kaiser test after Boc deprotection and it was estimated to be 59 μmol g^{-1}, proving that the PEG chain was successfully grafted onto GO (Fig. 3a). For the carboxylation procedure, GO **2** was mixed with chloroacetic acid in the presence of 3 M sodium hydroxide under bath sonication following the protocol described above, leading to GO **3** (Scheme 2). We cannot exclude that chloroacetic acid may also react with the secondary amine of the PEG chain introduced after the epoxide ring opening. However, the close proximity of this secondary amine with the surface of GO likely hampers such a derivatization due to steric

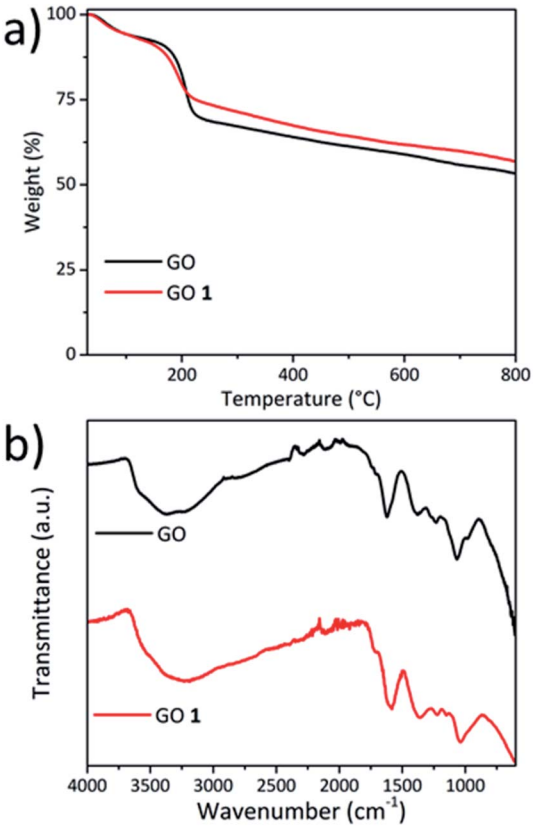

Fig. 2 (a) TGA of the pristine GO and GO **1** performed in an inert atmosphere. (b) FT-IR spectra of the pristine GO and GO **1**.

inaccessibility. The Kaiser test of GO **3** after Boc deprotection revealed that the amount of amines decreased to 14 μmol g^{-1} after the carboxylation (Fig. 3a), indicating that the PEG chain may be partially removed during the reaction due to the partial reduction of GO during the carboxylation step. GO **3** was further reacted with BocNH-PEG_{10}-NH_2 through amidation in the presence of EDC/NHS to give the double functionalized GO **4**. An increase of the amount of primary amines was measured by the Kaiser test (27 μmol g^{-1}), confirming that the PEG chain was linked to GO through amidation of the carboxyl groups (Fig. 3a). Meanwhile, a control reaction was performed by directly grafting BocNH-PEG_{10}-NH_2 on GO **2** through amidation obtaining GO **4-CTR** (Scheme S1†). The Kaiser test value (62 μmol g^{-1}) showed a little increase compared to GO **2** (Fig. 3a), thus confirming that there is only a limited amount of carboxyl groups at the edges of GO and that the reaction with chloroacetic acid allows more COOH moieties to be introduced on GO.

The removal of some functional groups during the carboxylation step due to the strongly basic conditions was confirmed by thermogravimetric analysis (Fig. 3b). Compared to the starting GO, GO **2** displayed another weight loss region located between 200 and 400 °C, corresponding to the degradation of the PEG chain bound to GO. However, GO **3** showed a higher thermal stability compared to GO **2**, probably due to the deoxygenation under strongly basic conditions. After the amidation reaction, more PEG chains were grafted onto the GO surface, resulting in a higher weight loss for GO **4** between 200 and 400 °C. Overall, the TGA results confirmed the successful double functionalization of GO thanks to the presence of the

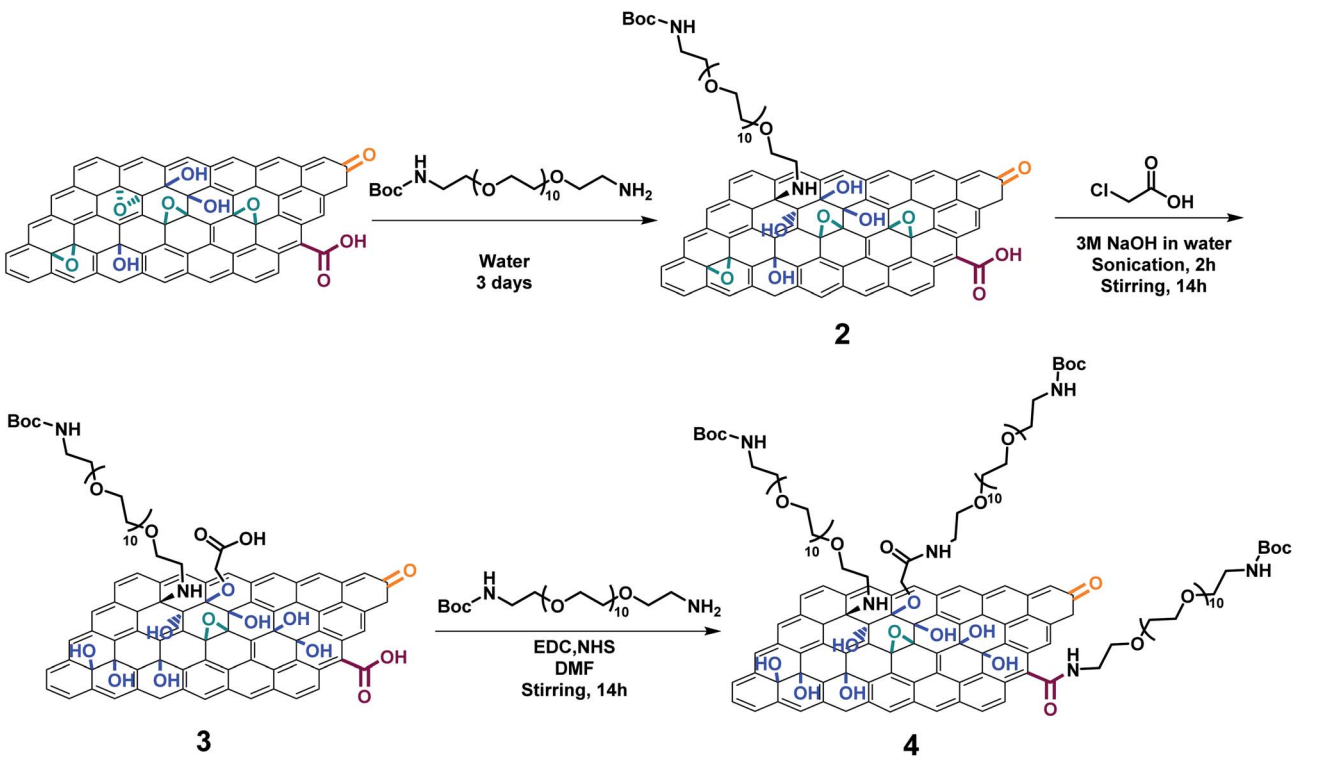

Scheme 2 Double functionalization of GO combining the epoxide ring opening reaction and the carboxylation reaction. For the sake of clarity, only one type of functional group is derivatized.

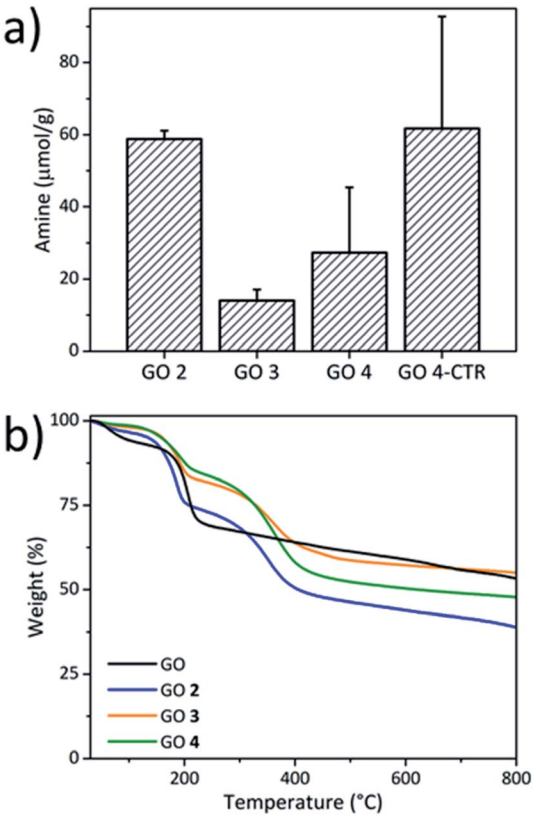

Fig. 3 (a) Kaiser test of GO **2**, GO **3**, GO **4** and GO **4-CTR**, and (b) TGA of the pristine GO, GO **2**, GO **3** and GO **4** performed in an inert atmosphere.

additional carboxyl groups. Nevertheless, the distinct thermal properties of GO **3** compared to GO **2** revealed that some functionalities were partially removed during the carboxylation step. The XPS analysis also confirmed the removal of some functional groups during the reaction (Fig. S3†). After the carboxylation step, the ratio of nitrogen atoms on GO **3** increased from 1.0% to 1.8% compared to GO **2** due to the partial deoxygenation on GO. After the amidation reaction, the %N in GO **4** increased to 2.1%, proving that more PEG chains were grafted onto the GO surface.

With a combined epoxide ring opening and carboxylation/amidation, a stepwise double GO functionalization was successfully achieved. But, the partial reduction of GO resulted in a lower efficiency of total functionalization and limited this method to a certain extent for further application.

(2) Carboxylation of GO using a reduced amount of sodium hydroxide

In order to limit the significant reduction of GO during the carboxylation, we repeated this reaction using a lower amount of sodium hydroxide. The carboxylation of GO was performed in a sodium hydroxide solution at different pH values, at pH 9 (10^{-5} M NaOH in water) and pH 13 (0.1 M aqueous NaOH), giving GO **5a** and GO **5b**, respectively (Scheme 3). Both samples were characterized by XPS (Fig. 4). However, based on the C 1s spectra, we could not observe an evident increase of the amount of carboxyl groups in both cases, indicating a lower efficiency of carboxylation. Moreover, the C–O component of GO **5a** decreased to 39.7% compared to the pristine GO (44.0%), revealing a slight reduction of GO at pH 9. The reduction was more pronounced in GO **5b** (35.0% C–O) due to the higher pH. These results are consistent with an increase of the C/O ratio calculated from the survey spectra, from 2.6 for the pristine GO to 2.8 for GO **5a** and 3.0 for GO **5b**.

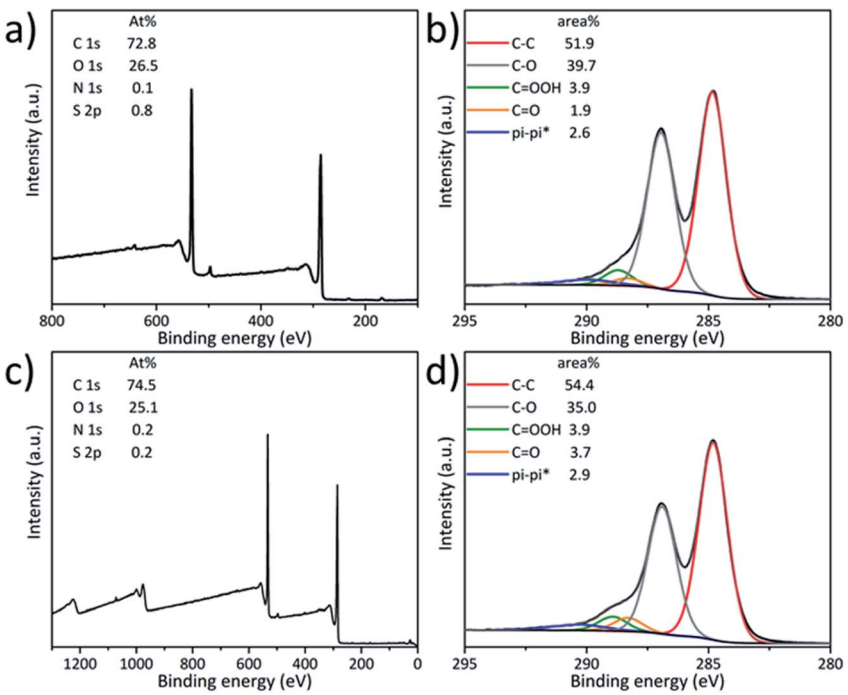

Fig. 4 XPS survey spectra (a and c) and high resolution C 1s (b and d) spectra of GO **5a** (top row) and GO **5b** (bottom row).

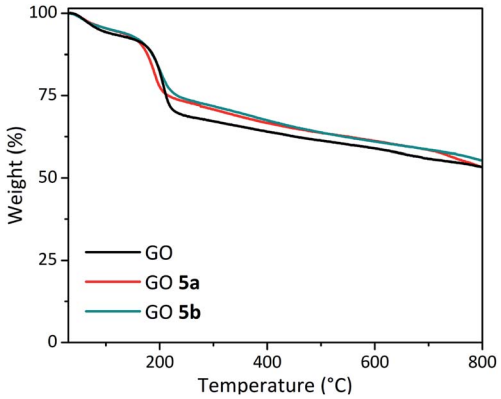

Fig. 5 TGA of the pristine GO, GO **5a** and GO **5b** performed in an inert atmosphere.

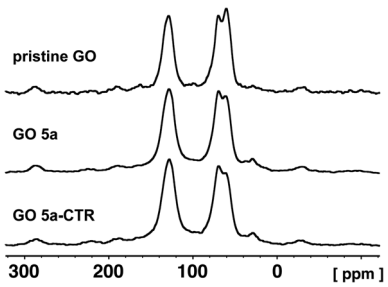

Fig. 6 ^{13}C DP/MAS NMR spectra of the pristine GO, GO **5a** and GO **5a-CTR**.

GO **5a** and GO **5b** were also characterized by TGA (Fig. 5). Both GO samples displayed a slightly higher thermal stability than the pristine GO at around 200 °C, which could be assigned to the removal of labile oxygen-containing groups. The TGA results are in agreement with the XPS data, showing a slight reduction of GO during the carboxylation step.

In order to clarify the low efficiency of the carboxylation reaction at lower pH, the pristine GO and GO **5a** were characterized by quantitative ^{13}C direct polarization (DP) solid state MAS-NMR (Fig. 6). A control reaction was also performed under the same conditions but without adding chloroacetic acid leading to GO **5a-CTR** (Scheme S2†). Detailed analysis of ^{13}C spectra required line shape fitting (Fig. S4†) with a CSA (Chemical Shift Anisotropy) model in order to get the intensities for inner components of each broad band (Table S1†). The ^{13}C NMR spectrum of GO confirmed the presence of abundant epoxides and hydroxyl groups with a strong band at 60.1 ppm and 69.8 ppm, respectively, and C=C bonds (peak at ~130 ppm).[29,51,52] The peak of the carboxyl groups around 164 ppm is negligible since the amount of carboxyl groups located at the edges of the pristine GO sheets is very low.[29] After the carboxylation reaction, unfortunately, the band of the carboxyl groups did not increase, confirming the inefficiency of the reaction at a lower pH.

The intensity of the peaks of the epoxides decreased from 22% in the pristine GO to 16% in GO **5a** and GO **5a-CTR**, while hydroxyls showed a little increase from 20% in pristine GO to 23% in GO **5a** and 22% in GO **5a-CTR**, respectively (Table S1†). The difference in the peak areas of the epoxides and the hydroxyls could be assigned to the opening of a small proportion of the epoxides by sodium hydroxide. The fitting of the C=C signal evidenced two peaks at *ca.* 126 and 132 ppm, which could be ascribed to graphitic localized clusters of C=C and to the other C=C in the proximity of oxygenated groups, respectively (Table S1†).

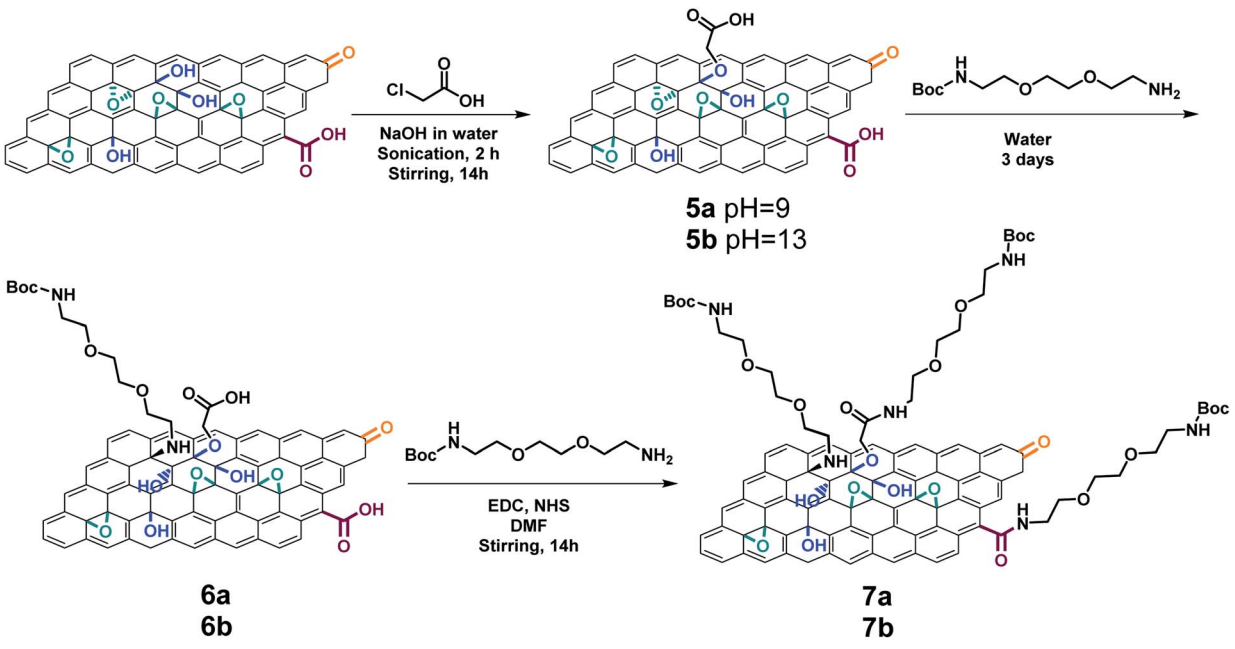

Scheme 3 Double functionalization of GO combining the carboxylation reaction using a reduced amount of sodium hydroxide and the epoxide ring opening reaction, followed by amidation. For the sake of clarity, only one type of functional group is derivatized.

Table 1 Percentage of nitrogen element and amount of amines on GO samples assessed by XPS and the Kaiser test, respectively

Sample	%N	Amine (μmol g^{-1})
5a	0.1	—
6a	1.3	105
7a	1.4	75
5b	0.2	—
6b	1.3	99
7b	1.4	75

To confirm whether more carboxyl groups were covalently linked onto the GO surface, the carboxylated GO samples prepared at pH 9 (GO **5a**) and pH 13 (GO **5b**) were derivatized with *N*-Boc-2,2′-(ethylenedioxy)diethylamine (Boc-TEG-NH_2) (Scheme 3). Since the reduction of GO was not severe at pH 9 and pH 13, we assumed it was possible to perform the carboxylation keeping the epoxide group which can be susceptible to the following ring opening reaction. The carboxylated GO **5a** and GO **5b** reacted first with Boc-TEG-NH_2 through a nucleophilic epoxide ring opening, giving GO **6a** and GO **6b**, respectively. Then, Boc-TEG-NH_2 was coupled to GO **6a** and GO **6b** by amidation with the carboxyl groups of GO, obtaining GO **7a** and GO **7b**.

The GO samples were characterized by XPS (Fig. S5†). A significant increase of the %N values was observed for GO **6a** and GO **6b**, indicating the successful functionalization of GO through epoxide ring opening (Table 1). However, the %N did not increase significantly after the amidation reaction, revealing that the amount of carboxyl groups on the GO surface was very low. These results were supported by the Kaiser test. After Boc deprotection, the amounts of primary amines in GO **6a** and GO **6b** were calculated as 105 and 99 μmol g^{-1}, respectively (Table 1). Both double functionalized GO **7a** and GO **7b** did not present a higher amount of amines due to the low efficiency of the carboxylation step at pH 9 and 13. The slight decrease of the amine level after the amidation was likely caused by the removal of some PEG chains physisorbed onto GO by DMF.

By applying this alternative strategy using a lower amount of sodium hydroxide, the reduction of GO was limited. Nevertheless, the carboxylation was not efficient, thus limiting the scope of the double functionalization strategy based on carboxylation followed by epoxide ring opening.

Conclusion

In summary, we investigated the influence of different amounts of sodium hydroxide on the carboxylation of GO aiming to prepare a multifunctional platform using controlled chemical approaches. The significant increase of the carboxyl groups on GO was observed only under strongly basic conditions, but a concomitant partial reduction of GO also occurred. Combining an epoxide ring opening, carboxylation and amidation reaction, GO was doubly functionalized, provoking, however, a significant reduction of the material accompanied by the removal of some functionalities during the carboxylation step. With a lower amount of sodium hydroxide, GO was not significantly reduced. Only a slight dehydration was observed due to a small proportion of the epoxides being opened by sodium hydroxide. Nevertheless, under these conditions, the introduction of carboxylates was negligible. Although it was possible to attach two distinct molecules by combining carboxylation with the epoxide ring opening reaction, the total level of functionalization remained lower than that of a direct epoxide ring opening. Overall, our results demonstrate that carboxylation is not an efficient approach for the functionalization of GO due to the partial reduction of GO and it can be hardly extended to achieve an efficient double functionalization of GO for further modifications. This work shows that it is very important to consider side reactions that may not be mentioned in the previous literature. The control of the derivatization of GO is crucial, in particular for biological purposes. The surface modification would tune the intrinsic properties of GO, affecting the loading efficiency and other factors which are important for its application in biosensing and disease treatment as drug nanocarriers.

Conflicts of interest

There are no conflicts to declare.

Acknowledgements

We gratefully acknowledge the support of the Centre National de la Recherche Scientifique (CNRS) through the International Research Project MULTIDIM between the I2CT Unit and Okayama University, the International Center for Frontier Research in Chemistry (icFRC), and financial support from the Agence Nationale de la Recherche (ANR) through the LabEx project Chemistry of Complex Systems (ANR-10-LABX-0026_CSC). SG is indebted to the Chinese Scholarship Council for supporting his PhD internship. We wish to thank Cathy Royer and Valérie Demais for help with TEM analyses at the "Plateforme Imagerie *in vitro*" at the Center of Neurochemistry (INCI, Strasbourg, France).

References

1 L. Zhang, Y. Ding, C. Zhang, Y. Zhou, X. Zhou, Z. Liu and G. Yu, *Chem*, 2018, **4**, 1035–1046.
2 U. R. Farooqui, A. L. Ahmad and N. A. Hamid, *Renewable Sustainable Energy Rev.*, 2018, **82**, 714–733.
3 X. Lu, X. Feng, J. R. Werber, C. Chu, I. Zucker, J. H. Kim, C. O. Osuji and M. Elimelech, *Proc. Natl. Acad. Sci. U. S. A.*, 2017, **114**, E9793–E9801.
4 M. Y. Xia, Y. Xie, C. H. Yu, G. Y. Chen, Y. H. Li, T. Zhang and Q. Peng, *J. Controlled Release*, 2019, **307**, 16–31.
5 F. Vulcano, A. Kovtun, C. Bettini, Z. Xia, A. Liscio, F. Terzi, A. Heras, A. Colina, B. Zanfrognini, M. Melucci, V. Palermo and C. Zanardi, *2D Mater.*, 2020, **7**, 024007.
6 D. K. Ji, C. Ménard-Moyon and A. Bianco, *Adv. Drug Delivery Rev.*, 2019, **138**, 211–232.

7 G. Reina, J. M. González-Dominguez, A. Criado, E. Vázquez, A. Bianco and M. Prato, *Chem. Soc. Rev.*, 2017, **46**, 4400–4416.
8 B. Jana, G. Mondal, A. Biswas, I. Chakraborty, A. Saha, P. Kurkute and S. Ghosh, *Macromol. Biosci.*, 2013, **13**, 1478–1484.
9 B. Jana, A. Biswas, S. Mohapatra, A. Saha and S. Ghosh, *Chem. Commun.*, 2014, **50**, 11595–11598.
10 B. Han, Y. L. Zhang, L. Zhu, Y. Li, Z. C. Ma, Y. Q. Liu, X. L. Zhang, X. W. Cao, Q. D. Chen, C. W. Qiu and H. B. Sun, *Adv. Mater.*, 2019, **31**, 1806386.
11 D. C. Marcano, D. V. Kosynkin, J. M. Berlin, A. Sinitskii, Z. Sun, A. Slesarev, L. B. Alemany, W. Lu and J. M. Tour, *ACS Nano*, 2010, **4**, 4806–4814.
12 W. S. Hummers and R. E. Offeman, *J. Am. Chem. Soc.*, 1958, **80**, 1339.
13 D. R. Dreyer, S. Park, C. W. Bielawski and R. S. Ruoff, *Chem. Soc. Rev.*, 2010, **39**, 228–240.
14 O. C. Compton and S. T. Nguyen, *Small*, 2010, **6**, 711–723.
15 G. P. Kotchey, B. L. Allen, H. Vedala, N. Yanamala, A. A. Kapralov, Y. Y. Tyurina, J. Klein-Seetharaman, V. E. Kagan and A. Star, *ACS Nano*, 2011, **5**, 2098–2108.
16 R. Kurapati, J. Russier, M. A. Squillaci, E. Treossi, C. Ménard-Moyon, A. E. Del Rio-Castillo, E. Vazquez, P. Samori, V. Palermo and A. Bianco, *Small*, 2015, **11**, 3985–3994.
17 H. Golmohammadi, E. Morales-Narváez, T. Naghdi and A. Merkoçi, *Chem. Mater.*, 2017, **29**, 5426–5446.
18 N. Cheeveewattanagul, E. Morales-Narváez, A.-R. H. A. Hassan, J. F. Bergua, W. Surareungchai, M. Somasundrum and A. Merkoçi, *Adv. Funct. Mater.*, 2017, **27**, 1702741.
19 D. Chai, B. Hao, R. Hu, F. Zhang, J. Yan, Y. Sun, X. Huang, Q. Zhang and H. Jiang, *ACS Appl. Mater. Interfaces*, 2019, **11**, 22915–22924.
20 G. Reina, N. D. Q. Chau, Y. Nishina and A. Bianco, *Nanoscale*, 2018, **10**, 5965–5974.
21 N. D. Q. Chau, G. Reina, J. Raya, I. A. Vacchi, C. Ménard-Moyon, Y. Nishina and A. Bianco, *Carbon*, 2017, **122**, 643–652.
22 S. S. Bhosale, E. Jokar, A. Fathi, C.-M. Tsai, C.-Y. Wang and E. W.-G. Diau, *Adv. Funct. Mater.*, 2018, **28**, 1803200.
23 C. Cao, R. Jin, H. Wei, W. Yang, E. M. Goldys, M. R. Hutchinson, S. Liu, X. Chen, G. Yang and G. Liu, *ACS Appl. Mater. Interfaces*, 2018, **10**, 33078–33087.
24 P. Ji, W. Zhang, S. Ai, Y. Zhang, J. Liu, J. Liu, P. He and Y. Li, *Nanotechnology*, 2019, **30**, 115701–115710.
25 M. Wang, R. Jamal, Y. Wang, L. Yang, F. Liu and T. Abdiryim, *Nanoscale Res. Lett.*, 2015, **10**, 370–381.
26 V. Georgakilas, J. N. Tiwari, K. C. Kemp, J. A. Perman, A. B. Bourlinos, K. S. Kim and R. Zboril, *Chem. Rev.*, 2016, **116**, 5464–5519.
27 F. Li, X. Jiang, J. Zhao and S. Zhang, *Nano Energy*, 2015, **16**, 488–515.
28 K. C. Mei, N. Rubio, P. M. Costa, H. Kafa, V. Abbate, F. Festy, S. S. Bansal, R. C. Hider and K. T. Al-Jamal, *Chem. Commun.*, 2015, **51**, 14981–14984.
29 I. A. Vacchi, C. Spinato, J. Raya, A. Bianco and C. Ménard-Moyon, *Nanoscale*, 2016, **8**, 13714–13721.
30 I. A. Vacchi, J. Raya, A. Bianco and C. Ménard-Moyon, *2D Mater.*, 2018, **5**, 035037.
31 S. Guo, Y. Nishina, A. Bianco and C. Ménard-Moyon, *Angew. Chem., Int. Ed. Engl.*, 2020, **59**, 1542–1547.
32 I. A. Vacchi, S. Guo, J. Raya, A. Bianco and C. Ménard-Moyon, *Chem.–Eur. J.*, 2020, **26**, 6591–6598.
33 D. He, X. He, K. Wang, Z. Zou, X. Yang and X. Li, *Langmuir*, 2014, **30**, 7182–7189.
34 R. Imani, S. Prakash, H. Vali and S. Faghihi, *Biomater. Sci.*, 2018, **6**, 1636–1650.
35 T. Yin, J. Liu, Z. Zhao, Y. Zhao, L. Dong, M. Yang, J. Zhou and M. Huo, *Adv. Funct. Mater.*, 2017, **27**, 1604620.
36 T. Jiang, W. Sun, Q. Zhu, N. A. Burns, S. A. Khan, R. Mo and Z. Gu, *Adv. Mater.*, 2015, **27**, 1021–1028.
37 X. Sun, Z. Liu, K. Welsher, J. T. Robinson, A. Goodwin, S. Zaric and H. Dai, *Nano Res.*, 2008, **1**, 203–212.
38 H. Wang, Q. Zhang, X. Chu, T. Chen, J. Ge and R. Yu, *Angew. Chem., Int. Ed. Engl.*, 2011, **50**, 7065–7069.
39 C. Chen, W. Kong, H. M. Duan and J. Zhang, *Phys. Chem. Chem. Phys.*, 2014, **16**, 12858–12864.
40 X. Fan, W. Peng, Y. Li, X. Li, S. Wang, G. Zhang and F. Zhang, *Adv. Mater.*, 2008, **20**, 4490–4493.
41 K.-W. Park, *J. Mater. Chem. A*, 2014, **2**, 4292–4298.
42 J.-L. Han, D. Zhang, W. Jiang, Y. Tao, M.-J. Liu, M. R. Haider, R.-Y. Ren, H.-c. Wang, W.-L. Jiang, Y.-C. Ding, Y.-N. Hou, B. Zhang, H.-Y. Cheng, X. Xia, Z. Wang and A.-J. Wang, *J. Membr. Sci.*, 2019, **576**, 190–197.
43 T. Taniguchi, S. Kurihara, H. Tateishi, K. Hatakeyama, M. Koinuma, H. Yokoi, M. Hara, H. Ishikawa and Y. Matsumoto, *Carbon*, 2015, **84**, 560–566.
44 P. Zhang, Z. Li, S. Zhang and G. Shao, *Energy Environ. Mater.*, 2018, **1**, 5–12.
45 M. Shams, L. M. Guiney, L. Huang, M. Ramesh, X. Yang, M. C. Hersam and I. Chowdhury, *Environ. Sci.: Nano*, 2019, **6**, 2203–2214.
46 J. P. Rourke, P. A. Pandey, J. J. Moore, M. Bates, I. A. Kinloch, R. J. Young and N. R. Wilson, *Angew. Chem., Int. Ed. Engl.*, 2011, **50**, 3173–3177.
47 A. M. Dimiev, L. B. Alemany and J. M. Tour, *ACS Nano*, 2013, **7**, 576–588.
48 T. Szabó, O. Berkesi and I. Dékány, *Carbon*, 2005, **43**, 3186–3189.
49 M. A. Lucherelli, J. Raya, K. F. Edelthalhammer, F. Hauke, A. Hirsch, G. Abellan and A. Bianco, *Chem.–Eur. J.*, 2019, **25**, 13218–13223.
50 E. Kaiser, R. L. Colescott, C. D. Bossinger and P. I. Cook, *Anal. Biochem.*, 1970, **34**, 595–598.
51 A. Lerf, H. He, M. Forster and J. Klinowski, *J. Phys. Chem. B*, 1998, **102**, 4477–4482.
52 W. Cai, R. D. Piner, F. J. Stadermann, S. Park, M. A. Shaibat, Y. Ishii, D. Yang, A. Velamakanni, S. J. An, M. Stoller, J. An, D. Chen and R. S. Ruoff, *Science*, 2008, **321**, 1815–1817.

